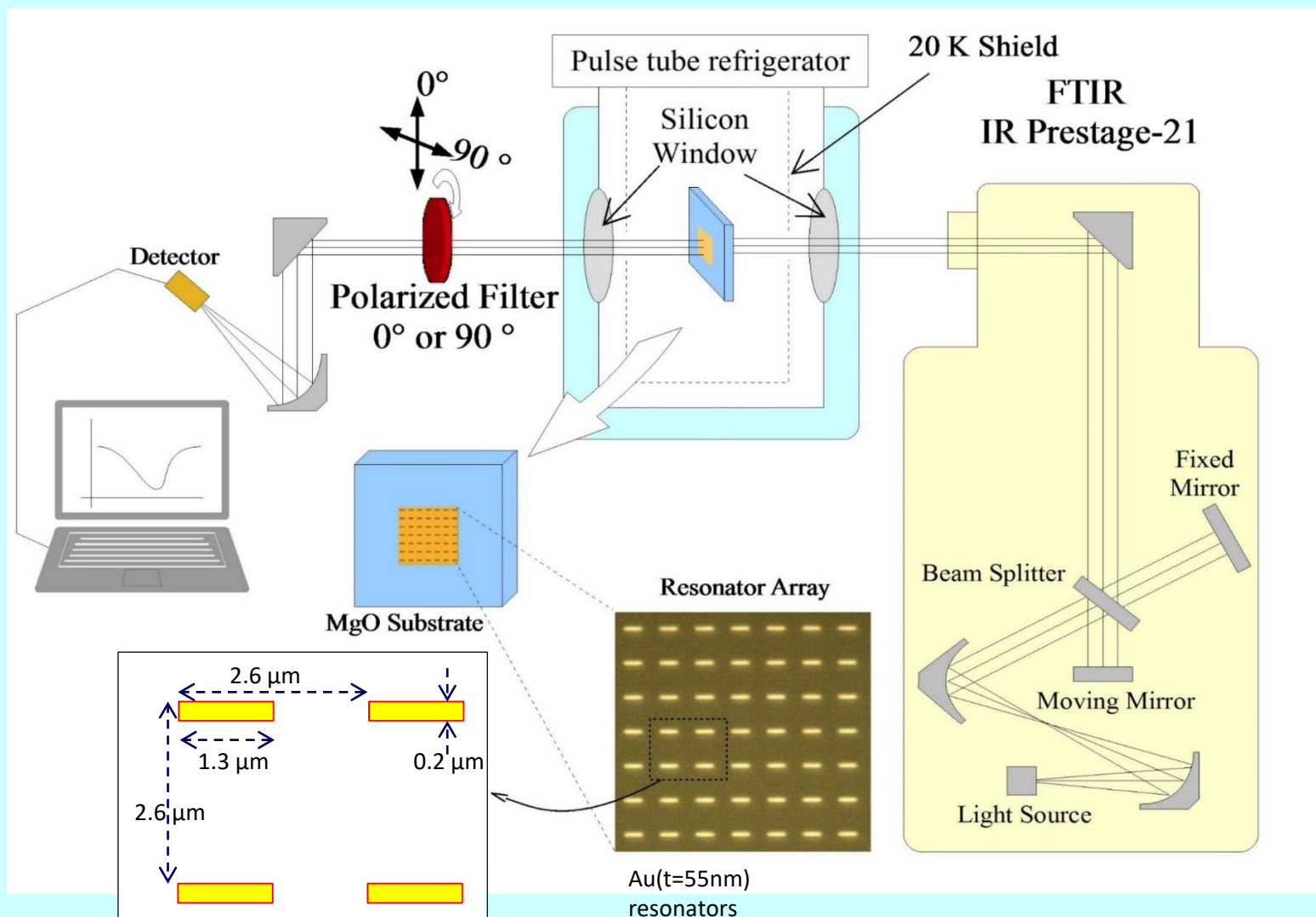


**Abstract** To design antennas for mid-infrared superconducting hot-electron bolometer (HEB), the surface reactance of Au thin film at cryogenic temperatures was evaluated using Fourier transform infrared spectroscopy with a sample cooling system. We fabricated mid-infrared resonator arrays that were constructed by gold thin film strips, and found that the resonant frequency was shifted to the low frequency side as the temperature was lowered. By fitting the resonant frequency to simulated results, the corrected surface reactance was established. Prototypes of a mid-infrared HEB formed by a twin-slot antenna with a niobium nitride strip were fabricated. When the HEB was biased close to the critical current under mid-infrared pulsed light ( $\lambda=4.89 \mu\text{m}$ ) irradiation, the detector output synchronized with the trigger signal was observed. The output waveforms comprised voltage pulse trains, and the full width at half maximum of the pulse was evaluated to be approximately 0.25 ns.

## I. Surface impedance correction of gold under cryogenic

Because of the mid infrared light range is at the region of occurrence of anomalous skin effect, the complex surface impedances of the Au films were needed for the simulation of MIR circuits. The impedances were derived using the measured refractive indices. However, these derivations were insufficient for designing superconducting MIR devices. Therefore, we corrected the surface impedance at cryogenic temperatures by using a FTIR with sample cooling system.



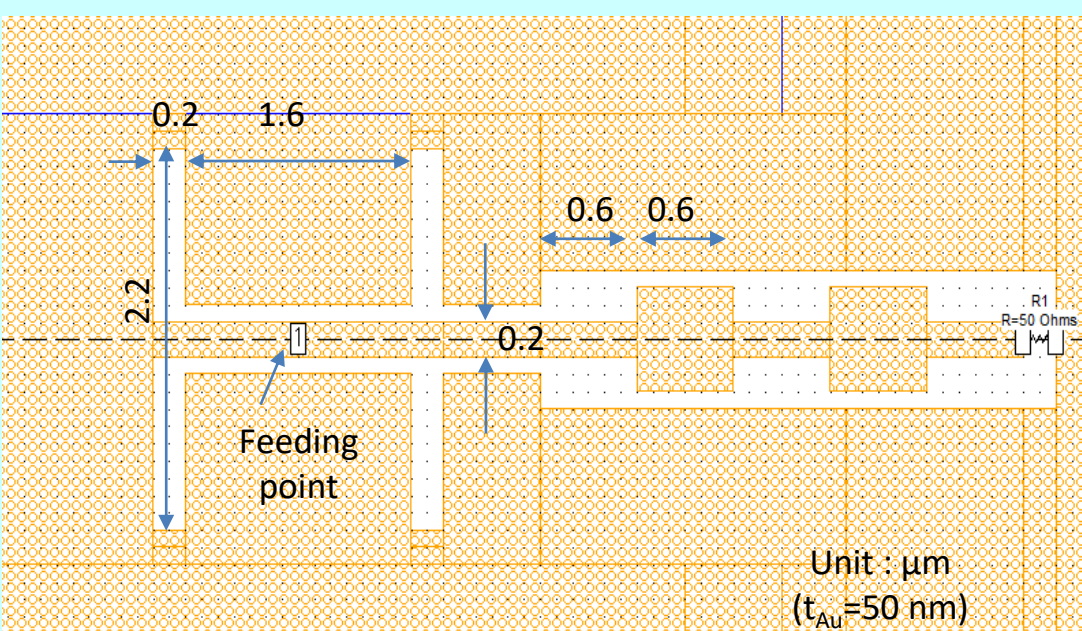
Fourier transform infrared spectroscopy with a sample cooling system.

For the evaluation, resonator arrays constructed of thin film strips of Au were fabricated. Their length and width were set at  $1.3 \mu\text{m}$  and  $0.2 \mu\text{m}$ , respectively, and were placed at intervals of  $2.6 \mu\text{m}$ . In the transmittance spectrum, the resonant frequency was observed as absorption properties at around  $2100 \text{ cm}^{-1}$  ( $63 \text{ THz}$ ). When the temperature changed from 200 K to 100 K, it was found that the resonant frequency shifted to the low frequency side. Simulations suggested that the shift of resonant frequency was mainly caused by a change in surface reactance. Therefore, we corrected the surface reactance and the correction value was found to be 1.6 times the surface reactance at room temperature.

## II. Design of mid-infrared twin-slot antenna with $X_s$ correction

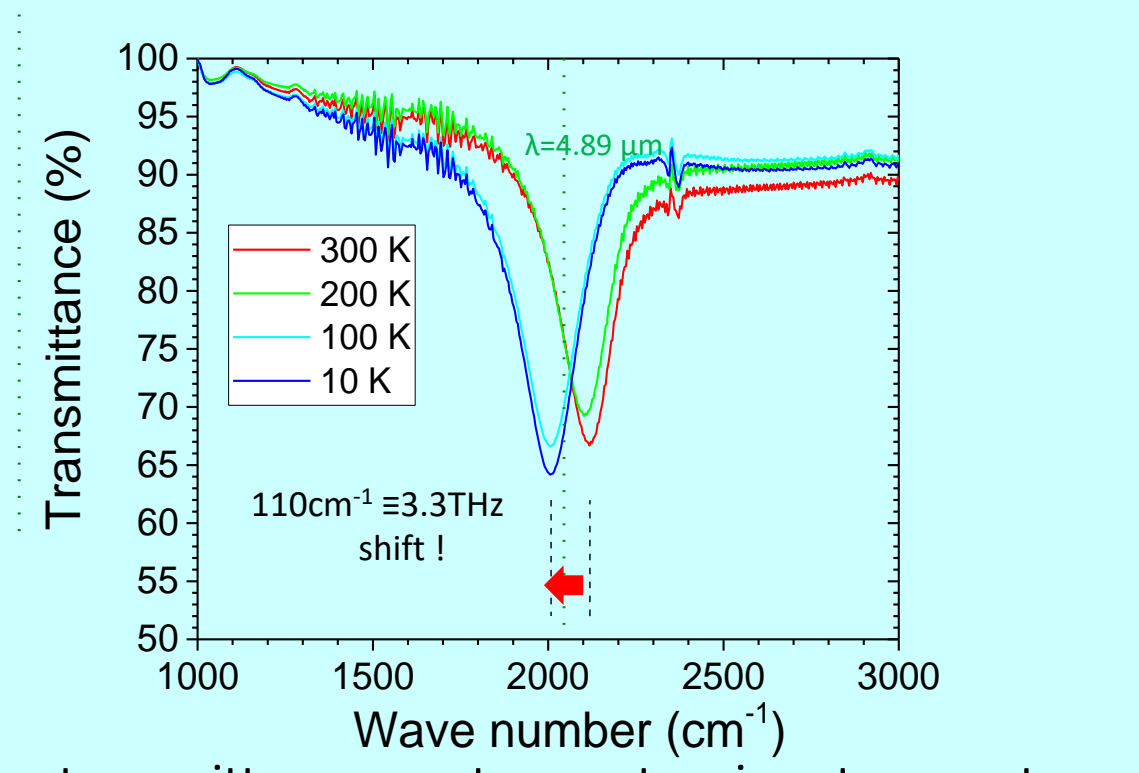
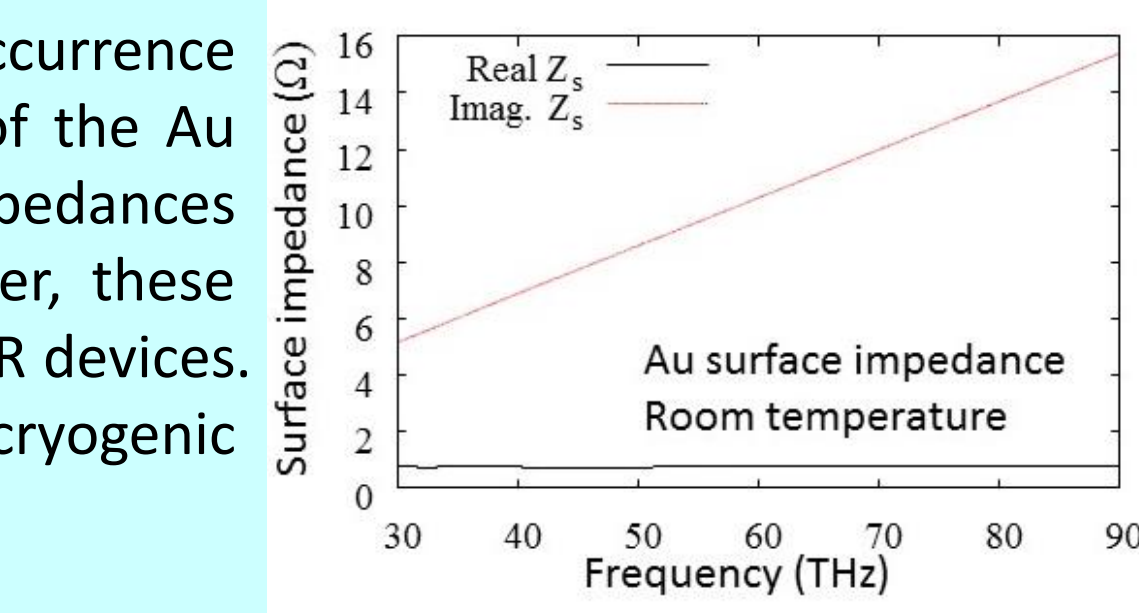
By using the corrected surface impedances, the antenna size was designed using the Sonnet EM simulator for operation at approximately 60 THz.

Designed frequency : 61.3 THz ( $\lambda=4.89 \mu\text{m}$ )



The design of the twin-slot antenna

The antenna was twin-slot antenna and the slot length and width were set at 2200 and 200 nm, respectively. The passive circuits were also decided by the simulator. At designed frequency of 61.3 THz, the antenna impedance was expected to be  $Z_{\text{Ant}} = 250 - j6 \Omega$ .



The transmittance spectra at various temperatures.

The surface reactance was corrected by fitting the resonant frequency to the simulated results.

$$Z_s = R_s + j1.6X_s \text{ @ } 61 \text{ THz, } T=100 \text{ K.}$$

## III. Fabrication of MIR HEBs with a twin-slot nano-antenna

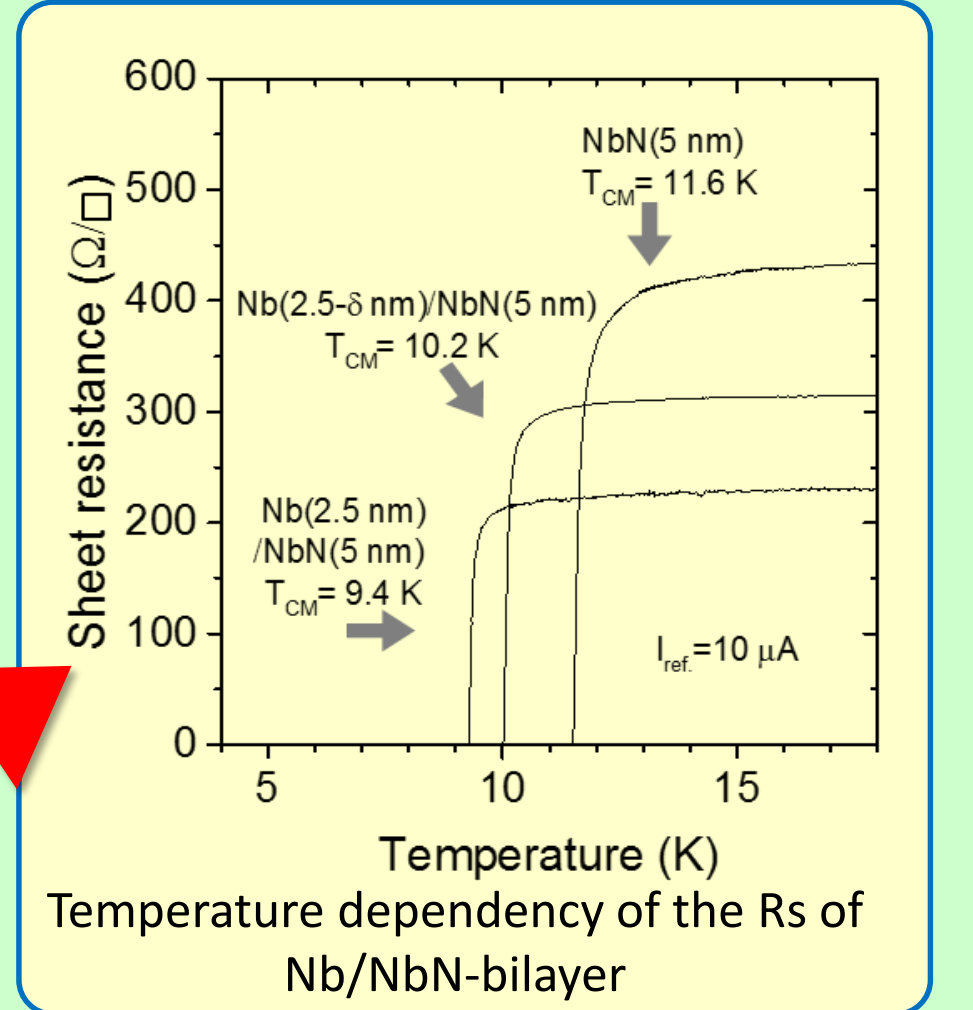
### 1. Study of MIR-HEBM structure using NbN

**Agenda 1.** It is necessary to reduce the sheet resistance of the superconducting thin film used for the superconducting strip. (The width of MIR-HEB is 1/10 of THz-HEB)

At first, we use a relatively thick NbN thin film of 7 nm.

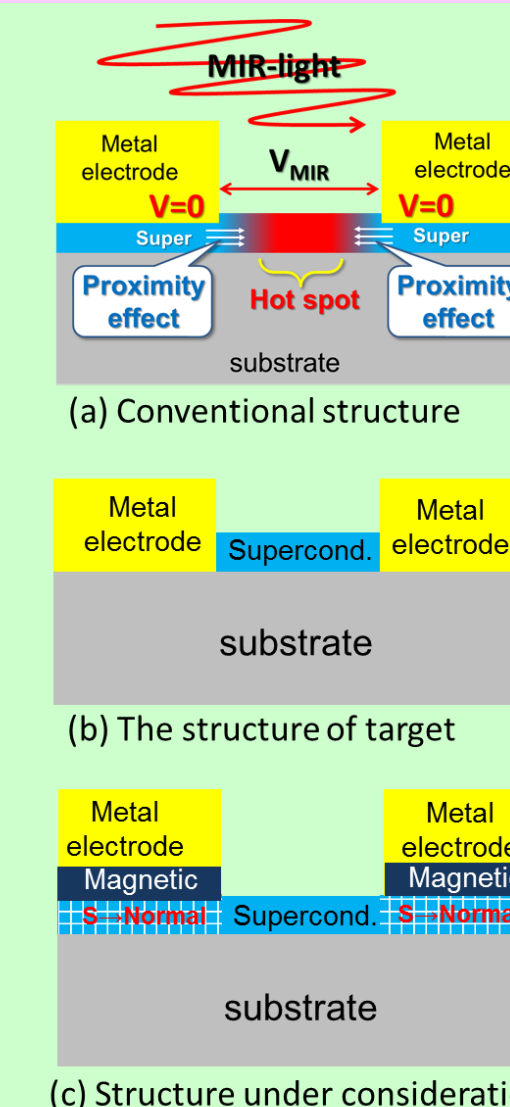
- The HEB resistance is still large (400-500  $\Omega$ )
- Large  $I_c$  (over 150  $\mu\text{A}$ )

Reduction of sheet resistance by using Nb/NbN bilayer



Temperature dependency of the Rs of Nb/NbN-bilayer

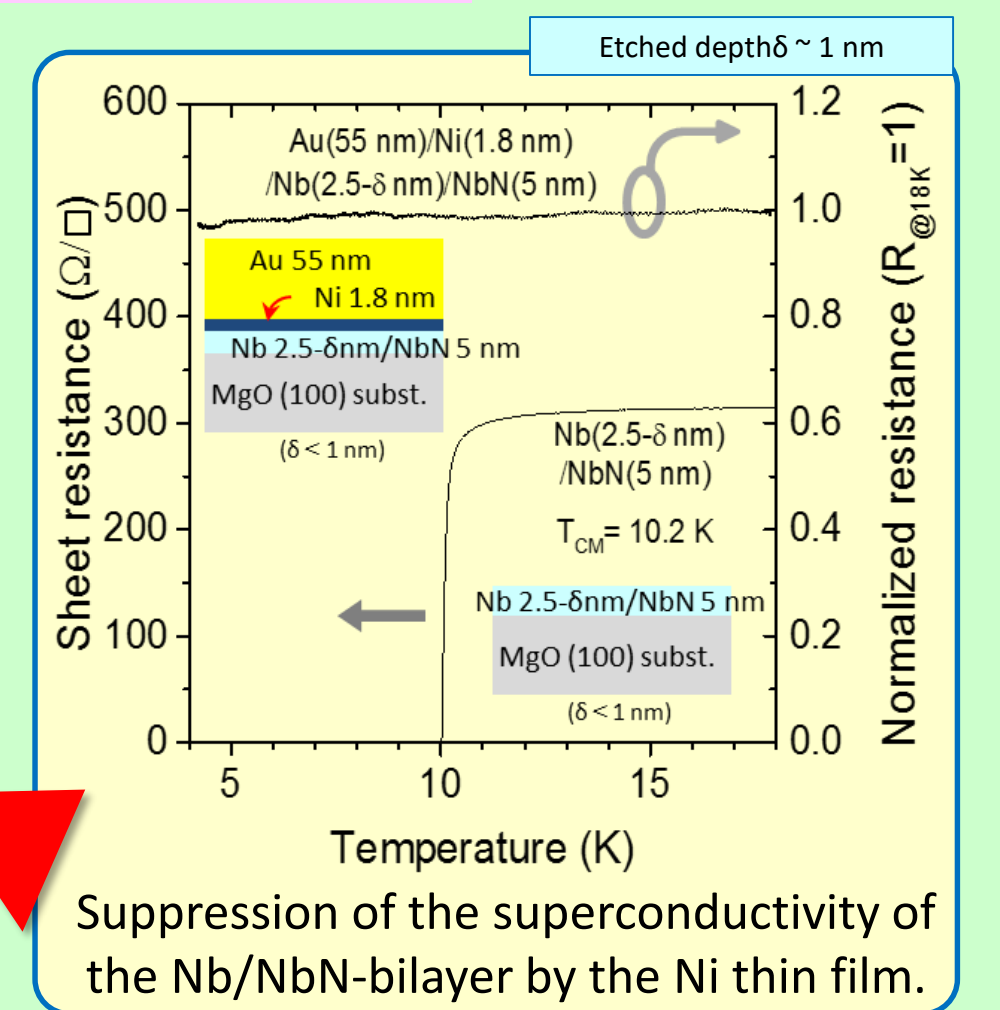
**Agenda 2.** Suppression of the superconductivity of the Nb/NbN layer by Ni thin film.



It is expected that Cooper pairs are injected into the hot spot region close to the superconducting region due to the proximity effect, which is undesirable such as a reduction in response to the incident signal (see fig(a)).

Since it is difficult to construct a superconducting strip only at the feeding point (see fig. (b)), we attempted suppression of superconductivity under the electrode by forming a magnetic thin film under the metal electrode (see fig. (c)).

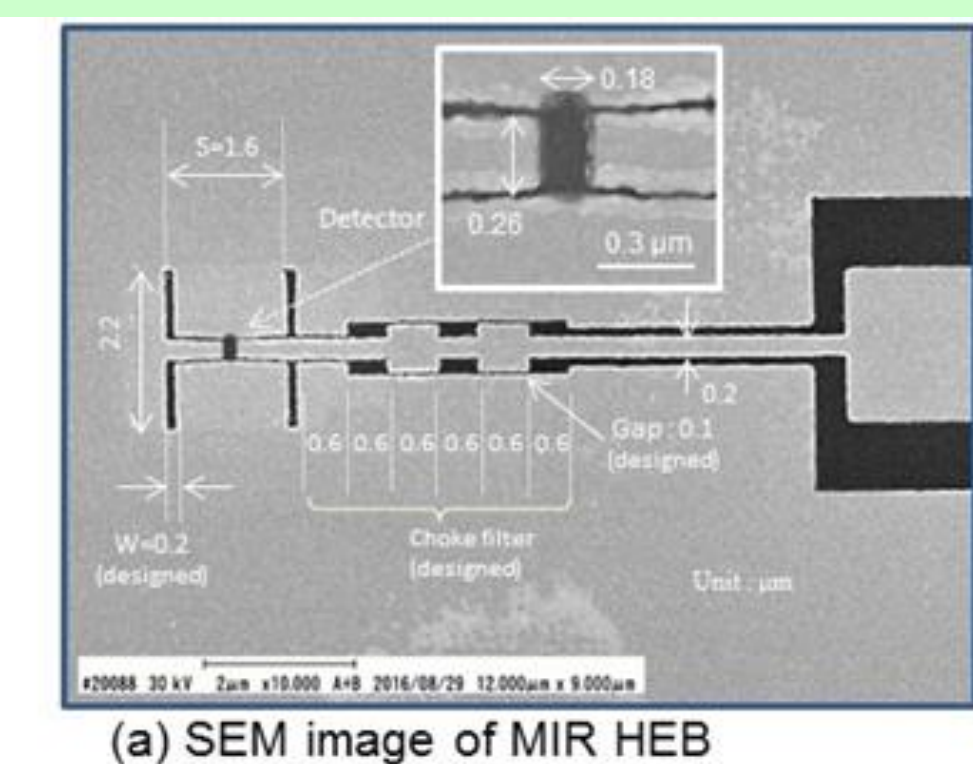
We found that superconductivity of Nb (2.5 - 8 nm) / NbN (5 nm) just below electrodes can be eliminated by adding an Ni thin film with a film thickness of 1.8 nm. In this case, the same electrode structure is adopted for MIR-HEBM fabrication.



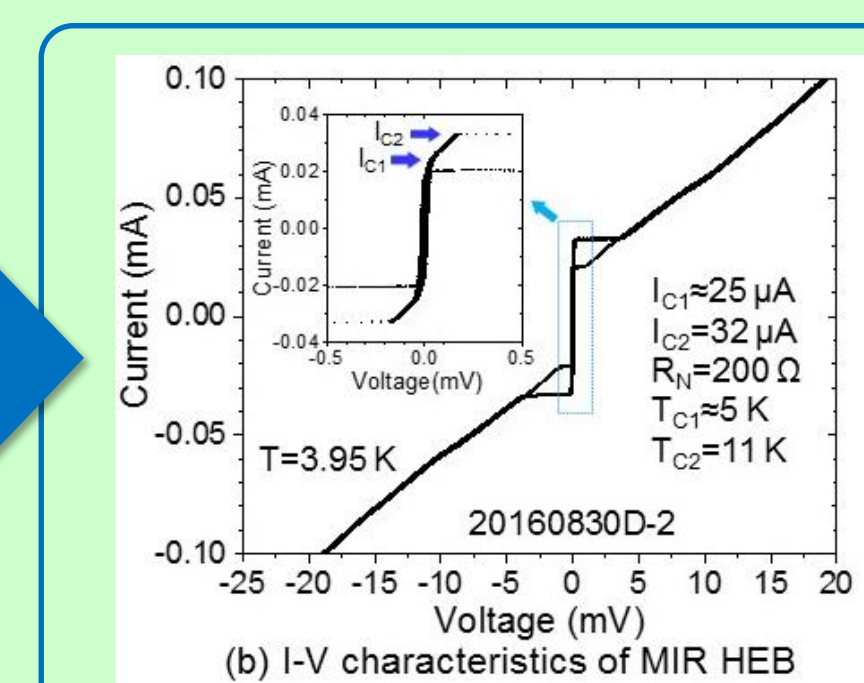
Suppression of the superconductivity of the Nb/NbN-bilayer by the Ni thin film.

### 2. Fabrication of MIR-HEBs

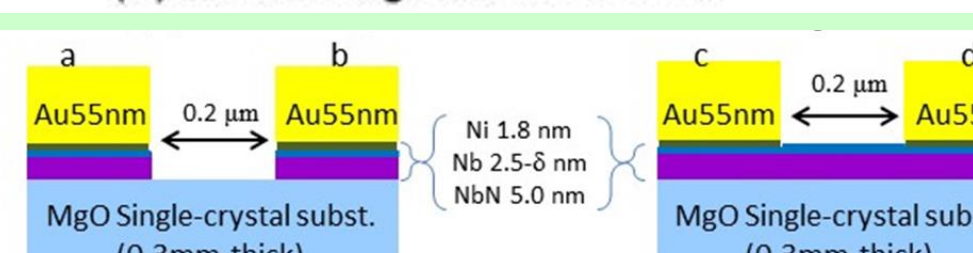
Fabricating the MIR HEBs with an antenna structure requires the building of fine structures on nano scales. We developed a new fabrication process using electron beam lithography for all of our lithography processes. To realize this process, two types of inorganic resists of NbN and MgO were used.



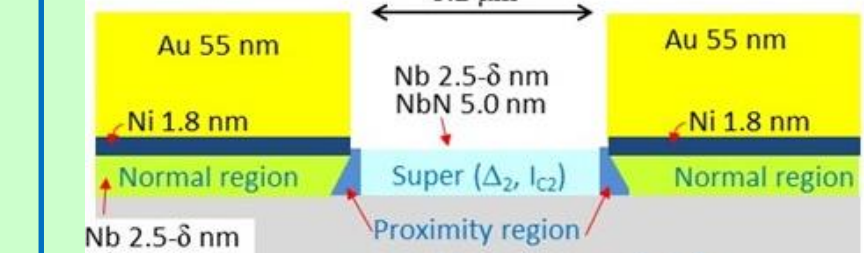
(a) SEM image of MIR HEB



(b) I-V characteristics of MIR HEB



(a) SEM image of the MIR HEB, (b) I-V characteristics of the HEB, (c) The schematics of the cross section of the HEB.



(a) SEM image of the MIR HEB, (b) I-V characteristics of the HEB, (c) The schematics of the cross section of the HEB.

The measured detector width and length were approximately 0.26 and 0.18  $\mu\text{m}$ , respectively. In the I-V characteristics, there are two critical currents ( $I_c$ ). We consider that there are two different superconductivity regions. One is the strip near the metal electrode affected by Ni, and the other is the region without the influence of Ni. Two transition temperatures associated with these 2 regions ( $T_{c1}$  and  $T_{c2}$ ) were observed at 5 K and 11 K. The measured normal resistance of the HEB was approximately 200  $\Omega$ .

## IV. Evaluation of MIR HEB detectors

### 1. Measurement setup for MIR-HEB Mixers

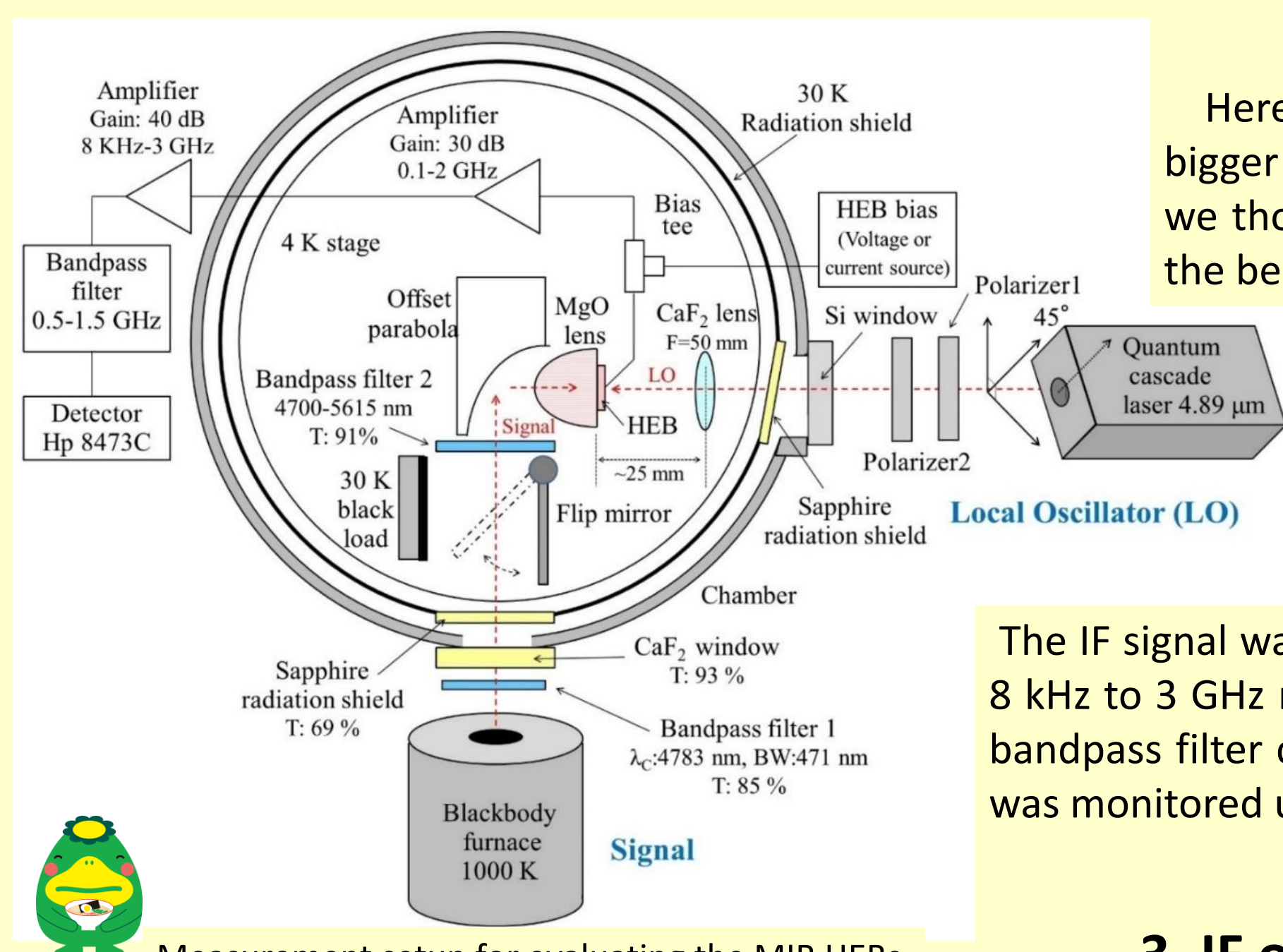
A mid-infrared quantum cascade laser (QCL) was used as the local oscillator. Here, the wavelength was 4.89  $\mu\text{m}$ . The polarization of the LO was dictated by "Polarizer 2". Certainly, the antenna gain directivity is strong substrate side, but it remains also on the vacuum side. In MIR region, the dielectric constant of MgO was reduced to be about 2.66. Radiation power ratio of the substrate direction  $P_d$  and the vacuum direction  $P_v$  of the slot antenna formed on a thick dielectric substrate can be expressed as follows[ref]:

$$P_d = \epsilon_d \frac{3}{2} P_v$$

Here, using  $\epsilon_{\text{MgO}}=2.66$ , the ratio of  $P_d/P_v=0.23$ . This is same or bigger than the reflection of the ordinary beam splitter. Therefore, we thought that, it is possible to use the vacuum side gain to avoid the beam splitter loss. [ref] Infrared and Millimeter Waves, Vol. 10, Part 1, p.18.

A black body furnace set at 1000 K was used as a reference signal. The total transmittance of the two bandpass filters and two windows in the signal input optical path was estimated to be about 50%.

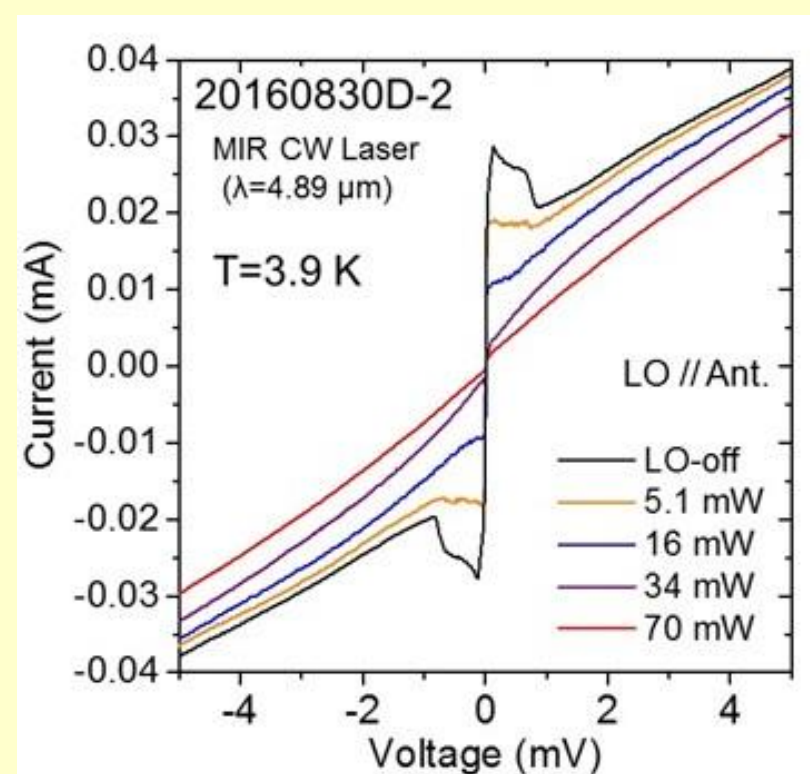
The IF signal was amplified by a 0.1-2 GHz cooled low-noise amplifier and an 8 kHz to 3 GHz room temperature amplifier. The signal was then filtered by a bandpass filter centered at 1 GHz with bandwidth of 1 GHz and the IF power was monitored using a Schottky diode detector.



Measurement setup for evaluating the MIR HEBs

### 2. The I-V characteristics of the MIR HEB

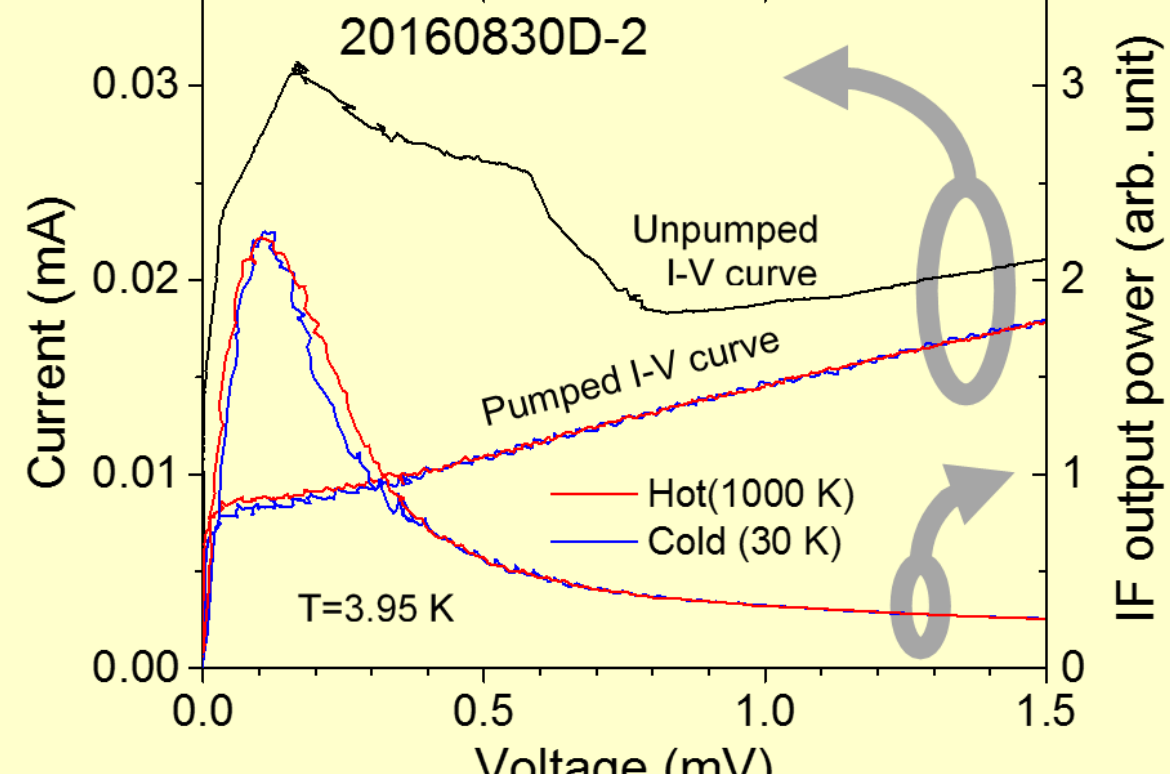
$I_c$  was suppressed to almost zero by LO irradiation, and it was found that sufficient power can be given to HEBM even with LO irradiation from the space side.



The LO-power dependency of the I-V characteristics.

### 3. IF output power characteristics

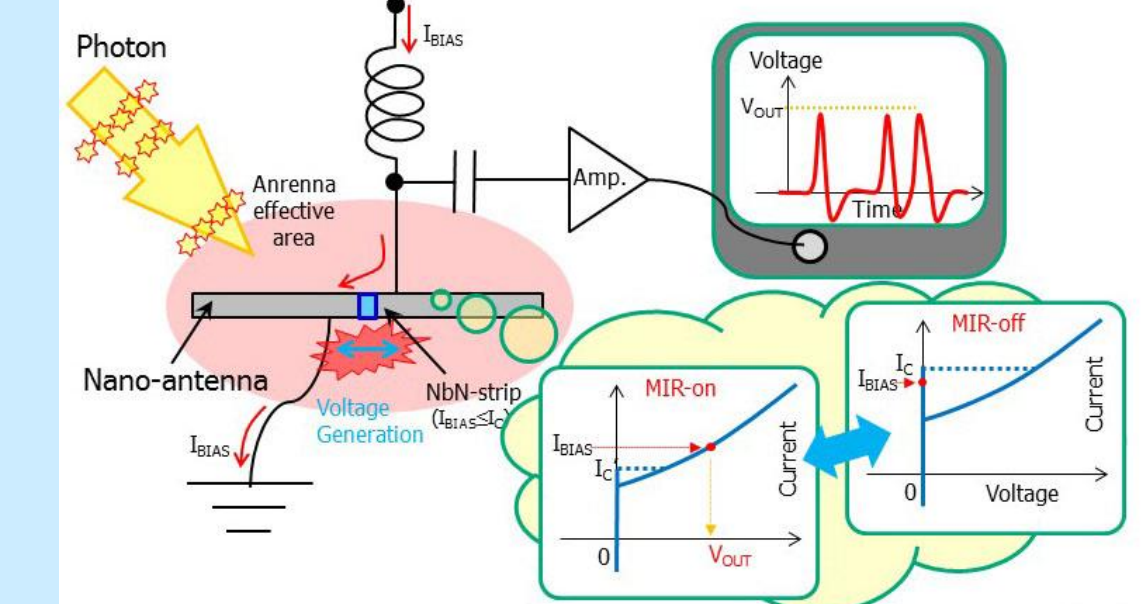
The periodic noise caused by the vibration of the GM refrigerator was observed in the IF output characteristics, and the obvious difference of the IF output power between 1000 K and 30 K thermal loads have not been confirmed.



I-V and IF output power characteristics of the MIR HEB as a function of bias voltage.

## V. Output waveform of the HEB under pulsed MIR-light irradiation.

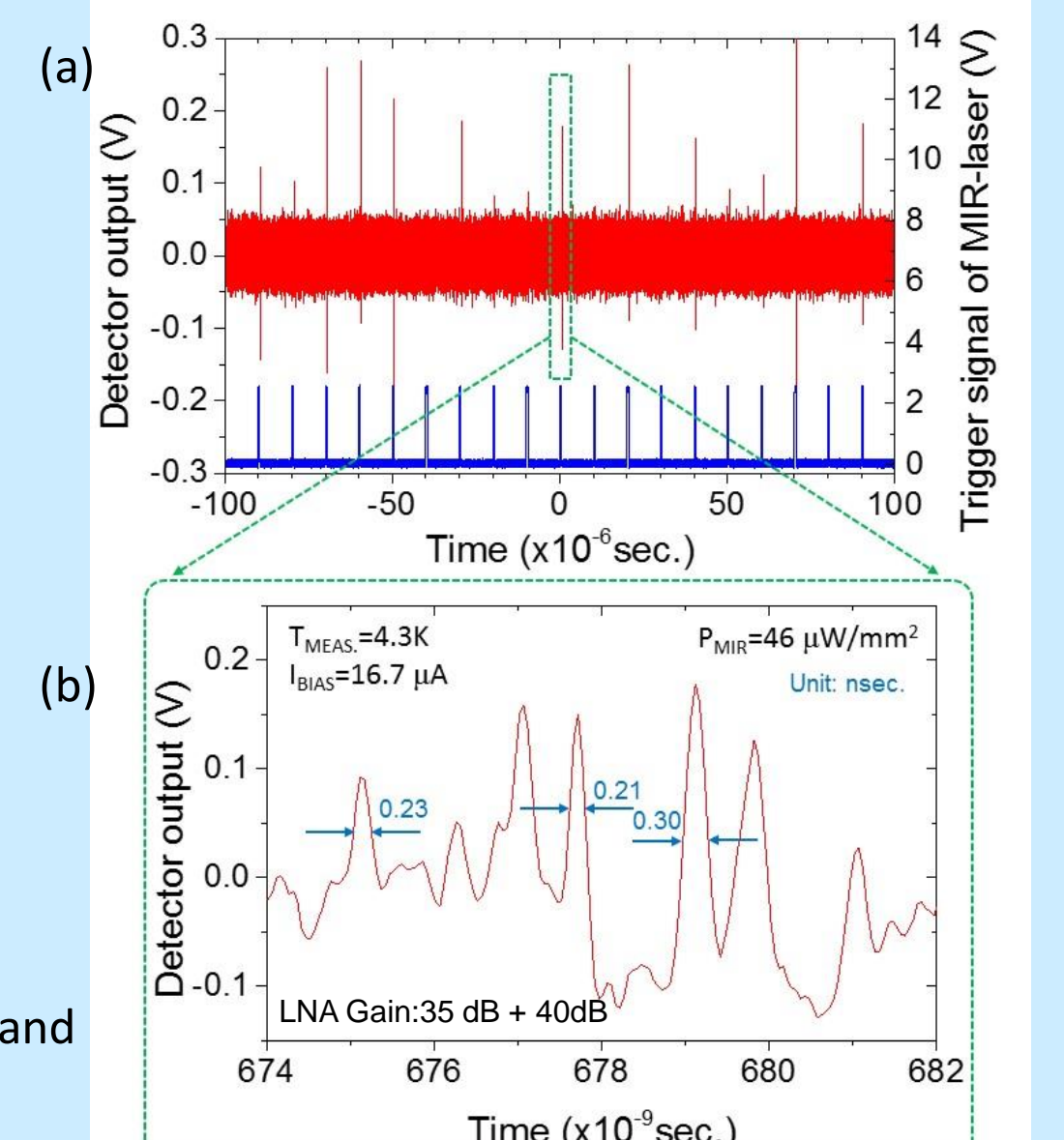
### 1. Operation of the superconducting mid-infrared detector



First, the HEB is biased close to  $I_c$ . By the irradiation of mid-infrared light, the electron temperature will be increased and  $I_c$  will be reduced. When the  $I_c$  is reduced less than the bias current, the output voltage will be observed.

### 2. Output waveform of the HEB under pulsed MIR-light irradiation.

Under the condition that the incident light was sufficiently attenuated so that the HEB element is not saturated, the detector output was observed to be synchronized with the trigger signal when the HEB was biased close to  $I_c$ . The detector showed an output voltage synchronized with the irradiation pulse light. In addition, the individual output voltage waveform was a voltage pulse train having a half width of approximately 0.25 ns.



Responses of the MIR HEB for pulsed light irradiation (a) and Output waveform of the MIR HEB (b)

### 3. Output waveform under CW-MIR-light irradiation.

Due to fluctuation of the continuous wave (CW) of MIR light, the pulse output which was averaged by 4096 pulses was also observed under constant bias. The obtained full width at half maximum of the pulse was about 0.21 ns.

